RSC Advances

PAPER

Cite this: *RSC Adv.*, 2016, **6**, 4936

# Interaction of Cd(II) and Ni(II) terpyridine complexes with model polynucleotides: a multidisciplinary approach†

G. Barone,[a] G. Gennaro,[a] A. M. Giuliani[a] and M. Giustini*[b]

Received 24th November 2015
Accepted 23rd December 2015

DOI: 10.1039/c5ra24919h

www.rsc.org/advances

Two metal complexes of 2,2′:6′,2″-terpyridine (terpy), *i.e.* Cd(terpy)$Cl_2$ and Ni(terpy)$Cl_2 \cdot 3H_2O$, have been prepared and extensively characterized. The interaction of Cd(terpy)$Cl_2$ with synthetic DNA models, poly(dA-dT)·poly(dA-dT) (polyAT) and poly(dG-dC)·poly(dG-dC) (polyGC), has been studied by CD, fluorescence and UV-vis electronic absorption spectroscopy at several metal/polynucleotide–phosphate ratios and for different NaCl concentrations. All the experimental results indicate an intercalative mechanism of interaction. The optimized geometry of the cadmium complex intercalated between the sixth and seventh base pairs of (AT) and (GC) dodecanucleotide duplexes, obtained by quantum mechanics/molecular mechanics (QM/MM) calculations, lends support to the proposed mechanism. The calculated models provide some additional structural details of the intercalation complex at the molecular level. To evidence the influence of the charge and geometry of the metal complex on the mechanism of interaction with polynucleotides, the nickel complex–polyAT system has been studied to some extent by means of CD and UV-vis spectroscopy, and by thermal melting experiments. The results suggest that the octahedral complex cation $[Ni(terpy)(H_2O)_2Cl]^+$ interacts with polyAT by partial intercalation assisted by electrostatic interaction with the negative charges of the backbone phosphate groups.

## Introduction

Small molecules can interact non-covalently with the DNA double helix by several mechanisms: electrostatic interactions with the negatively charged sugar–phosphate backbone, groove-binding, that causes little perturbation of the DNA structure, and intercalation, *i.e.* insertion of planar chromophores between adjacent base-pairs. The interaction between DNA and metal complexes with potential biological activity is of particular interest and is the focus of extensive investigation.[1–6]

Intercalation, at variance with electrostatic interactions and groove binding, causes important modifications of the DNA double helix. Indeed, it is accompanied by an increase of the rise of the helix, that involves changes of the twist angle and distortions in the sugar–phosphate backbone. Metallo-intercalators can act as dual-function complexes, binding both through the metal and through intercalation of the attached aromatic ligand.[5,6]

2,2′:6′,2″-Terpyridine (terpy: Scheme 1) was prepared for the first time by Morgan and Burstall in the 1930s.[7] The molecule and its derivatives contain three nitrogen atoms and, therefore, are among the N-heterocycles which have very high binding affinity towards metal ions due to dπ–pπ* back bonding of the metal to the pyridine rings and the chelate effect. Complexation of one or two terpy molecules can lead to metal-complexes, and in many cases bis-complexes, that may have different coordination geometries, as octahedral [particularly with ruthenium(II) and rhodium(III)], square-planar [particularly with platinum(II)], or trigonal bipyramidal [as for zinc(II) or copper(II)]. These compounds have been studied as potential diagnostic and anticancer agents, through intercalation between base pairs of DNA. For example, platinum terpyridine complexes bind DNA essentially by intercalation, with a binding constant of the order of $10^5$–$10^6$ $M^{-1}$, while the values for ruthenium(II) and copper(II) derivatives are generally lower by an order of magnitude.[8–12]

Among the many known metal complexes of terpyridine, we got particularly interested in those of Cd(II) and Ni(II), and in their interaction with model DNAs, as an extension of our studies on the poly(dA-dT)·poly(dA-dT) (briefly polyAT) and poly(dG-dC)·poly(dG-dC) (briefly polyGC) interactions with the $Cd^{2+}$ and $Ni^{2+}$ cations.[13–15] The synthesis of a Cd(II)–terpyridine

[a]*Dipartimento STEBICEF, Università di Palermo, 90128 Palermo, Italy*
[b]*Dipartimento di Chimica, Università "La Sapienza", P.le Aldo Moro 5, 00185 Roma, Italy. E-mail: mauro.giustini@uniroma1.it*

† Electronic supplementary information (ESI) available: Synthesis and characterization of the metal complexes; FT-IR spectra (Fig. S1) and band assignments (Table S1); thermogravimetric analysis (Table S2); electronic spectra (Fig. S2 and Table S3); supplementary CD and UV-Vis data (Fig. S3–S6); fluorescence supplementary data (Fig. S7–S10); QM/MM supplementary data (Table S4; Cartesian coordinates files: 1_dGC12.xyz – 1_dAT12.xyz – 2_dAT12.xyz). See DOI: 10.1039/c5ra24919h

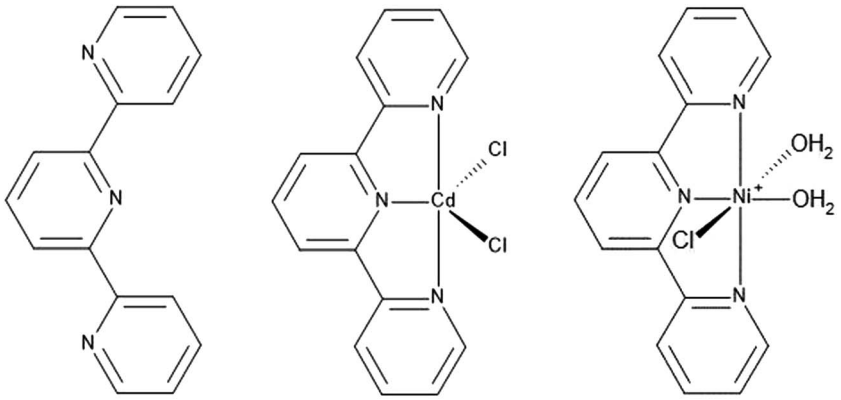


Scheme 1 Schematic representation of the 2,2′:6′,2″-terpyridine ligand, (a); of the Cd(terpy)$Cl_2$ complex (**1**), (b); of the $[Ni(terpy)(H_2O)_2Cl]^+$ complex (**2**), (c).

complex was first reported by Morgan and Burstall,[16] who proposed for the complex the formula [CdCl(terpy)]Cl, with the suggestion that its constitution would probably be more complicated than indicated by such formula. A distorted trigonal bipyramidal geometry has been proposed for Cd(terpy)$Cl_2$,[17,18] though an X-ray study[19] reports a square pyramidal arrangement for the complex. Bis-terpyridine complexes of Cd(II) have been reported containing substituted terpyridines, and essentially for the preparation of metallo-polymers with special properties.[20–22]

Both mono- and bis-terpyridine complexes of Ni(II) have been prepared and characterized.[23–26] The mono-terpyridine complex has been prepared in two forms, one anhydrous and the other containing $H_2O$ as ligand and/or of hydration. The golden yellow crystals of Ni(terpy)$Cl_2$, where the metal is penta-coordinated, readily absorb water from a moist atmosphere.[27,28] The hydrated nickel complex has been formulated as $[Ni(terpy)(H_2O)_2Cl]Cl\cdot H_2O$, based on X-ray diffraction data.[24] Many bis-terpyridine complexes of Ni(II), generally involving substituted terpyridines, have been synthesized, characterized and investigated, mainly for their interest in the preparation of metallo-supramolecular polymers.[29,30]

The Cd(II) and Ni(II) terpyridine complexes, though not novel, have never been fully characterized and studies on their interaction with DNA are completely absent. In the following, we will describe and discuss the synthesis, the physico-chemical characterization of Cd(II) and Ni(II) complexes with terpy and the results of their interactions with two synthetic models of DNA, namely polyAT and polyGC, studied by several spectroscopic techniques and by quantum mechanics/molecular mechanics (QM/MM) calculations. The joint use of an experimental and a theoretical approach is certainly the winning strategy to face the problem of the interaction of metal complexes with polynucleotides. The spectroscopic techniques used to define the interactions of both complexes with polynucleotides are the best to give an overall picture of these systems, being highly complementary and sensitive to different aspects of the interactions. An analogous approach has been recently successfully employed by our group to unravel the mechanism of interaction of the anticancer antibiotic doxorubicin with model polynucleotides and DNA.[31]

The study here presented appears significant in the framework of the problems to be faced in the design of new metal-based drugs, having DNA as a target, more selective and with reduced undesired side effects, since it broadens the experimental and theoretical background on the drugs/DNA interactions.

## Results

Cd(terpy)$Cl_2$ (complex **1**) is scarcely soluble in water, as expected for a neutral complex. On the contrary, the nickel–terpyridine complex $[Ni(terpy)(H_2O)_2Cl]Cl\cdot H_2O$ (complex **2**) is very soluble in water. Details on their synthesis and characterization *via* FT-IR, thermogravimetric and elemental analysis as well as their electronic spectra are reported in the ESI material (Fig. S1 and S2, Tables S1–S3†).

### Interaction of Cd(terpy)$Cl_2$ with polynucleotides

**Circular dichroism and absorption studies.** The interaction of complex **1** with polyAT was studied in several experimental conditions, *i.e.* fixed NaCl concentration and variable *R* (=[metal]/[polynucleotide−phosphate]) at different salt concentrations. UV-vis and circular dichroism spectra were acquired for the different samples. *R* was varied between 0 and 1.5 and the salt concentrations employed were 0, 2, 10 and 20 mM. Tris buffer 1 mM at pH 7.5 ± 0.3 was always employed. A typical set of CD spectra is shown in Fig. 1 for the system in 1 mM Tris–2 mM NaCl solution and *R* changing from 0.0 to 1.5 by titration of the polyAT solution with a concentrated solution of complex **1**.

The most prominent feature of these CD spectra is the presence of an evident ICD (Induced Circular Dichroism) signal

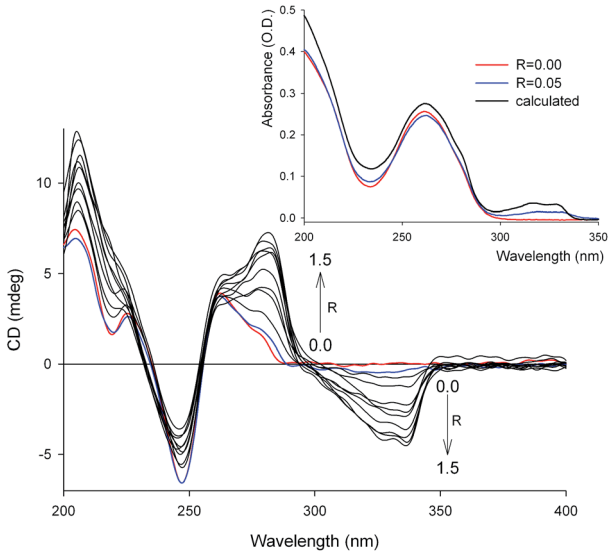


Fig. 1 CD spectra of polyAT titrated with **1**: $[polyAT]_P = 37.5\ \mu M$; $l = 1.0$ cm; $T = 298$ K. The inset shows the experimental UV spectra (same colours as in the main graph) and that obtained as the sum of polyAT spectrum and that of **1** at the same nominal concentrations as in the blue spectrum (see text for further details).

in the region where only the achiral terpyridine complex absorbs and not the polynucleotide. Conspicuous spectral modifications were observed also in the region between 260 and 300 nm. Similar spectral changes with $R$ were observed also in the absence of NaCl, while they became progressively less marked as the salt concentration was increased to 10 and 20 mM (spectra not shown), indicating a non-covalent type of interaction, involving also an electrostatic contribution.[32,33] Keeping these results in mind, most of the subsequent measurements on the polyAT–Cd(terpy)$Cl_2$ system were performed in 1 mM Tris–2 mM NaCl solution. The presence of ICD signals, that have a magnitude of less than 10 $M^{-1}$ $cm^{-1}$ (in $\Delta\varepsilon$ units) and correspond to the absorption bands of the bound and not of the free terpyridine complex, strongly suggested intercalation as the major mechanism of interaction.[32–36] The same indication comes from the electronic absorption spectra: the marked hypochromism of the polynucleotide band centred at 260 nm, and the red shift and hypochromism of the terpyridine band in the 300–350 nm region (inset of Fig. 1) upon interaction of the complex with polyAT are characteristic of intercalation.[34,36–38]

To investigate a larger range of $R$ values, titration of Cd(terpy)$Cl_2$ in 1 mM Tris–2 mM NaCl solution with polyAT was also performed. The essential features of the CD and UV-vis absorbance spectra (Fig. S3 – ESI,† for CD spectra), diagnostic for intercalation, *i.e.* presence of ICD with a magnitude of less than 10 $M^{-1}$ $cm^{-1}$ and the spectral position of the absorption bands of the bound terpyridine complex, hypochromism and bathochromic shift of the UV-vis bands of the metal complex, are preserved. However, the CD spectra obtained in the two types of titration for the same value of $R$ are different.

The interaction of **1** with polyGC was also investigated: CD and UV-Vis spectra in 2 mM NaCl–1 mM Tris solution were recorded titrating both the complex with polyGC and polyGC with **1** in order to explore a large $R$ interval. The 2 mM salt concentration was chosen because most of the data with polyAT had been collected in these conditions. The titration of polyGC with Cd(terpy)$Cl_2$, with $R$ changing from 0.1 to 2, gave the CD spectra shown in Fig. 2a. The spectra of the titration of Cd(terpy)$Cl_2$ with polyGC, for $R$ changing from 5 to 0.1 is shown in Fig. 2b. The two series, thus, have in common a considerable $R$ interval, but the spectra are very different, as already observed, though to a more limited extent, for polyAT. The CD spectrum of polyGC was markedly modified upon addition of the complex (Fig. 2a), and, most interestingly, ICD signals appeared at $\lambda >$ 300 nm increasing with $R$. At variance, titration of **1** with polyGC (Fig. 2b) only gave rise to CD spectra reminiscent of those of C-DNA or unwound B-DNA,[15,39–41] but with no sign of ICD. For comparison, complex **1** was also titrated with calf thymus DNA (ct-DNA) in 1 mM Tris–2 mM NaCl. The relevant CD spectra (Fig. S4 – ESI†) exhibit a clear ICD of the expected magnitude for an intercalative mode of binding.

**PolyAT melting experiments.** Intercalation should cause a marked increase of the melting temperature, $T_m$, of the intercalated polynucleotide,[32,42,43] and thus the thermal stability of polyAT in the presence of complex **1** was investigated

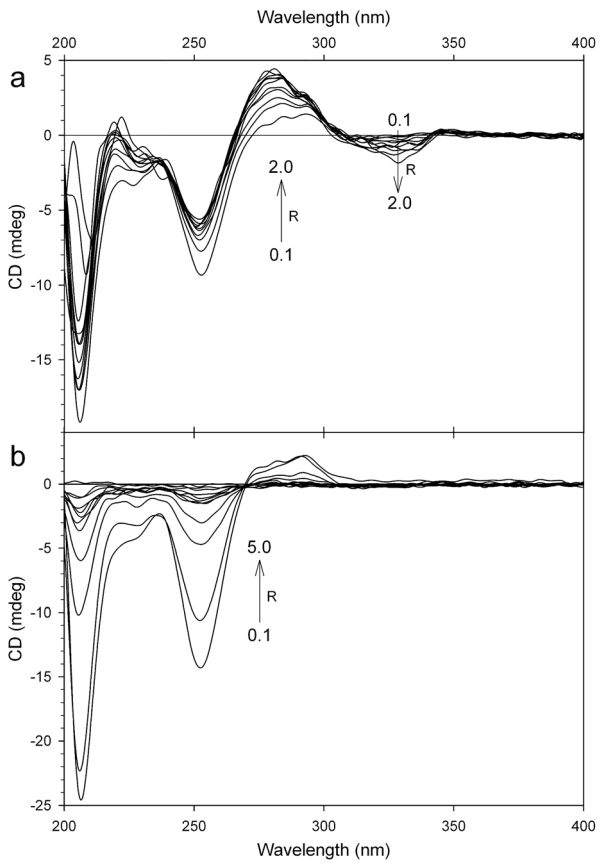


Fig. 2 Titration of polyGC with **1** (panel a; $[polyGC]_P = 50.6\ \mu M$) and of **1** with polyGC (panel b; $[\mathbf{1}] = 6.25\ \mu M$). $l = 1.0$ cm; $T = 298$ K.

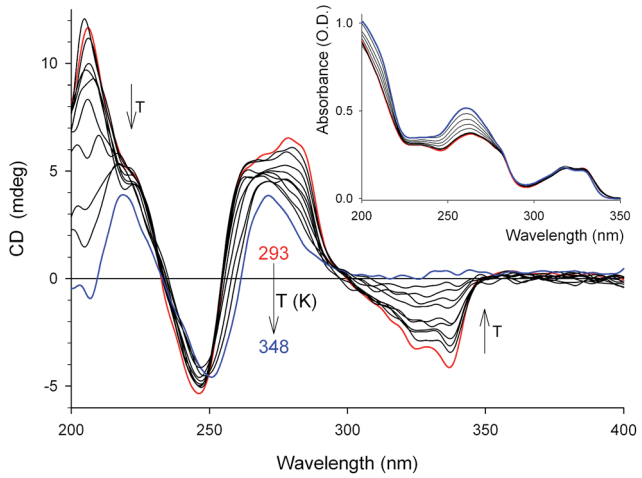


Fig. 3 CD spectra of the system **1**–polyAT at $R = 0.3$ as a function of temperature (in colour, the first and last spectrum of the series). The inset shows the corresponding UV spectra (colours as in the main graph). $[polyAT]_P = 43.5$ μM; $l = 1.0$ cm.

recording the variable temperature CD and UV-Vis spectra at several $R$ values and for NaCl concentrations 0, 2, 10 and 20 mM in Tris 1 mM. The CD spectra of a typical melting experiment are shown in Fig. 3 for NaCl 2 mM and $R = 0.3$ (in the inset the corresponding UV-Vis spectra). Melting not only entailed the disappearance of all ICD at $\lambda > 300$ nm, but also of the spectral alterations in the region below 300 nm, where polyAT absorbs. The thermal transition was perfectly reversible, namely the CD and UV-vis spectra recorded at a temperature well below $T_m$, before and after melting were identical (Fig. S5 – ESI†). Melting curves were obtained by plotting the absorbance at 260 nm and the CD at fixed wavelengths against the temperature (some representative melting curves are given in Fig. S6 – ESI†). The $T_m$ values are collected in Table 1. No thermal melting experiments were performed with polyGC, because of its too high melting temperature.

**Quantum mechanics/molecular mechanics calculations.** QM/MM calculations have been performed to support, at molecular level, the intercalative interaction of **1** with polyAT and polyGC as deduced by the experimental evidences. The optimized geometries of the intercalation complexes between **1** and the two dodecanucleotide models are shown in Fig. 4 and 5, respectively. Besides intercalation, additional stabilizing interactions occur between the Cd(II) complex and both polynucleotides. Moreover, substantial and interesting differences can be noticed in the binding with polyAT and polyGC, respectively.

The calculated models show short distances between the Cd(II) ion of **1** and the carbonyl oxygen of thymine and guanine, respectively for polyAT and polyGC (highlighted in red in the Fig. 4 and 5), the Cd–O distance being shorter for polyAT than for polyGC. Moreover, two additional hydrogen bonds are formed, in the complex with polyGC, between the two chlorido ligands and two amine hydrogen atoms of two cytosine bases (Cl–H distances of 2.44 and 2.21 Å, respectively). Such hydrogen-bond interactions, with the analogous amine hydrogens of adenine, are remarkably weaker in the complex with polyAT (Cl–H distances of 2.70 and 2.81 Å, respectively).

**Fluorescence studies.** The interaction between Cd(terpy)$Cl_2$ and the synthetic polynucleotides polyAT and polyGC was followed also with fluorescence spectroscopy. Indeed, Cd(terpy)$Cl_2$, in 1 mM Tris–2 mM NaCl buffer solution, when excited at 280 nm, exhibits a relatively intense fluorescence spectrum, characterized by two well defined maxima at 336 nm and 350 nm, together with a barely appreciable shoulder at 365 nm. The emission spectrum shows the expected mirror shape, compared to the absorption spectrum, with a Stokes shift in the range 10–20 nm (Fig. S7 – ESI†).

Upon addition of either polynucleotide to a Cd(terpy)$Cl_2$ solution in the same buffer, a strong quenching of the fluorescence is observed without modification of the emission bands' position (Fig. 6 and 7, for polyAT and polyGC,

Table 1 Melting temperatures (±half dispersion, K) of polyAT in the presence of Cd(terpy)$Cl_2$ for different $R$ values ($R = [1]/[polyAT]_P$)

| | [NaCl] (mM) | | | |
|---|---|---|---|---|
| $R$ | 0 | 2 | 10 | 20 |
| 0.0[a] | [b] | 305.1 | 317.5 | 322.8 |
| 0.1 | 317.3 ± 0.6 | 324.0 ± 0.1 | 321.3 ± 0.2 | 324.9 ± 0.2 |
| 0.2 | 323.7 ± 1.1 | | 322.7 ± 0.4 | |
| 0.3 | | 328.7 ± 0.4 | | |
| 0.5 | 333.6 ± 0.3 | 332.7 ± 0.2 | 328.1 ± 1.1 | 326.3 ± 0.1 |
| 0.7 | 334.4 ± 0.3 | | 330.4 ± 0.1 | |
| 1.0 | 328.6 ± 0.7 | 333.4 ± 0.8 | 331.8 ± 0.5 | 327.4 ± 0.2 |
| 1.5 | 328.7 ± 1.4 | 326.2 ± 0.2 | 334.7 ± 0.4 | |

[a] From ref. 44. [b] Melted at room temperature.

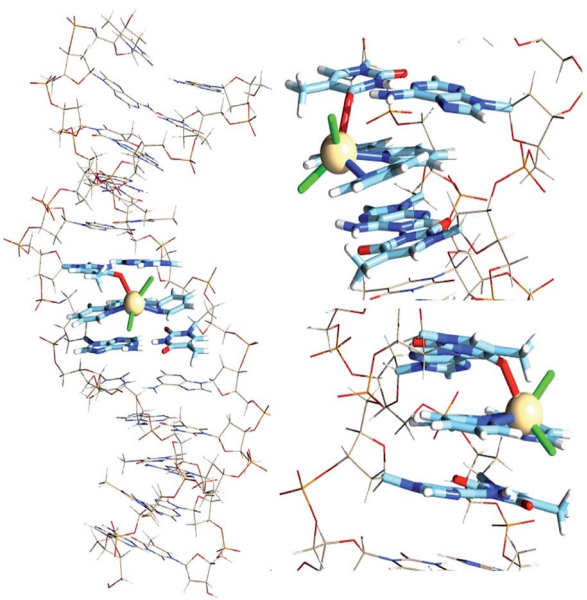

Fig. 4 Front and enlarged side views of the Cd(terpy)$Cl_2$/$d(ATATATATATAT)_2$ intercalation complex, whose geometry was optimized by QM/MM calculations (1_dAT12.xyz; ESI†). High level and low level layers are shown as sticks and wires, respectively.

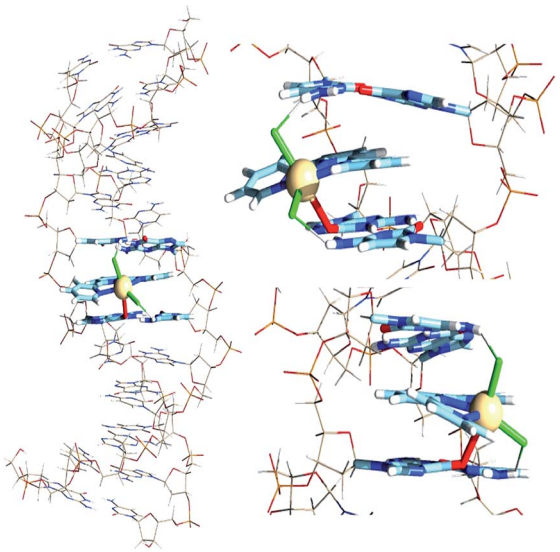

Fig. 5 Front and enlarged side views of the Cd(terpy)$Cl_2$/d(GCGCGCGCGCGC)$_2$ intercalation complex, whose geometry was optimized by QM/MM calculations (1_dGC12.xyz; ESI†). High level and low level layers are shown as sticks and wires, respectively.

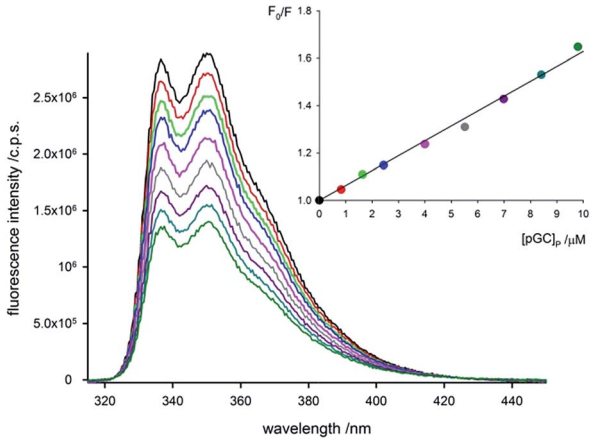


Fig. 7 Emission spectra of **1** (black curve) in the presence of increasing amounts of polyGC (coloured curves) ([**1**] = 4.3 μM; $l$ = 1.0 cm; $\lambda_{ecc}$ = 280 nm; slits 1.5/1.5 nm; $T$ = 298 K). The inset shows the Stern–Volmer plot obtained from the data of the main graph corrected for the absorbance of the solution[45] (colours refer to the spectra in the main graph; line is the best fit according to the Stern–Volmer relationship: $F_0/F = 1 + k_{SV}[\text{polyGC}]_P$; $k_{SV} = 6.3 \times 10^4$ $M^{-1}$).

respectively). Quenching follows the linear trend predicted by the Stern–Volmer relationship (see insets in Fig. 6 and 7). In order to gain details on the quenching process (whether static or dynamic), fluorescence lifetimes measurements were performed (Fig. S8–S10 – ESI†). Cd(terpy)$Cl_2$, in Tris–NaCl buffer at room temperature, shows a fluorescence decay with an average lifetime $\langle\tau\rangle$ of 1.33 ± 0.03 ns for both emission peaks (336 nm and 350 nm), that does not change along the titrations with either polynucleotide, strongly indicating the static nature of the quenching, *i.e.* the polymer–Cd(terpy)$Cl_2$ complex forms in the ground state and the quenching is not the deactivation of the excited state, but simply the formation of a non-fluorescent adduct.

These data point to a strong intercalative interaction between the metal complex and both polynucleotides with formation of a non-fluorescent species. Therefore, the measured fluorescence should be considered as due only to the metal complex free in solution.

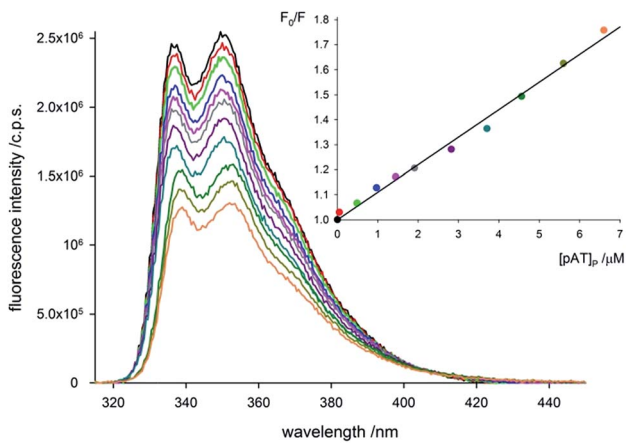


Fig. 6 Emission spectra of **1** (black curve) in the presence of increasing amounts of polyAT (coloured curves) ([**1**] = 3.8 μM; $l$ = 1.0 cm; $\lambda_{ecc}$ = 280 nm; slits 1.5/1.5 nm; $T$ = 298 K). The inset shows the Stern–Volmer plot obtained from the data of the main graph corrected for the absorbance of the solution[45] (colours refer to the spectra in the main graph; line is the best fit according to the Stern–Volmer relationship: $F_0/F = 1 + k_{SV}[\text{polyAT}]_P$; $k_{SV} = 1.1 \times 10^5$ $M^{-1}$).

### Interaction of [Ni(terpy)$(H_2O)_2$Cl]Cl·$H_2O$ with polyAT

The polyAT-[Ni(terpy)$(H_2O)_2$Cl]Cl·$H_2O$ system was studied to some extent essentially for the sake of comparison with the polyAT–Cd(terpy)$Cl_2$ one, to evidence possibly dissimilar interactions connected with the different geometry (octahedral *vs.* trigonal bipyramidal) and the different charge (positive *vs.* neutral) of the two complexes. The nickel system was examined at different $R$ values in 1 mM Tris–2 mM NaCl solution, since this had been found to be the most favourable salt concentration in the case of complex **1**. The results of a typical experiment, in which $R$ was changed from 8.4 to 0.5 by titration of **2** with polyAT are shown in Fig. 8. To explore the region of lower $R$ values (from 0.05 to 1.00) a series of samples was prepared by mixing a fixed volume (800 μL) of a 4.37 × $10^{-5}$ M solution of polyAT in 1 mM Tris–2 mM NaCl with increasing volumes of a 1.0 × $10^{-4}$ M solution of complex **2** in the same solvent and adding the Tris–NaCl buffer solution to a final volume of 1000 μL. The relevant CD spectra are shown in Fig. 9. Very significant alterations were observed in the region of $\lambda$ < 300 nm, while only very weak ICD signals appeared at higher wavelengths at all $R$ values, in contrast with the results obtained with **1** (see Fig. 1).

Variable temperature CD and UV-vis measurements were also performed on the polyAT–complex **2** system for $R$ values 0.1, 0.5 and 1.0, at NaCl concentrations 0, 2 and 10 mM in Tris 1 mM. Denaturation of the polynucleotide was observed in all experimental conditions considered; the melting temperatures

 

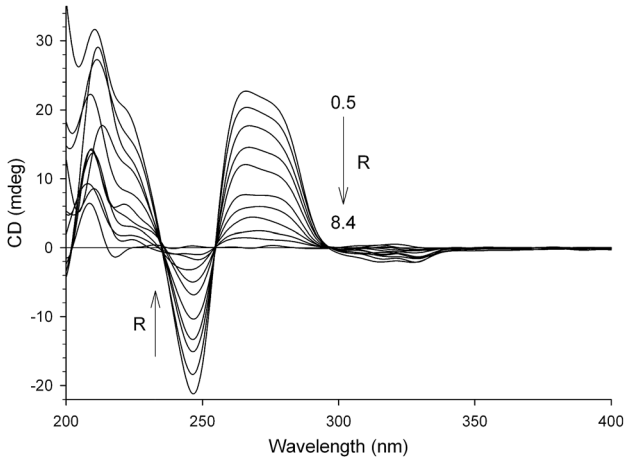


Fig. 8 CD spectra of the titration of **2** with polyAT ([**2**] = 70 μM; $l$ = 1.0 cm; $T$ = 298 K).

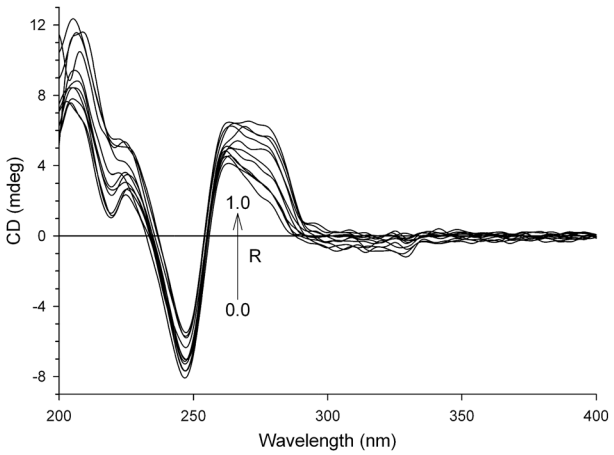


Fig. 9 CD spectra of the titration of polyAT with **2** ([polyAT]$_P$ = 35 μM; $l$ = 1.0 cm; $T$ = 298 K).

were obtained as above detailed for the complex **1**–polyAT system, and are collected in Table 2. A typical feature of the variable temperature UV-vis spectra (Fig. 10), not observed with the cadmium complex, was the decrease of absorbance and the red shift of the characteristic bands of the complex at $\lambda$ > 300 nm, giving rise to an isosbestic point at *ca.* 335 nm (depending

Table 2 Melting temperatures (±half dispersion, K) of polyAT in the presence of [Ni(terpy)($H_2O$)$_2$Cl]Cl·$H_2O$

| | NaCl (mM) | | |
|---|---|---|---|
| $R$ = [**2**]/[polyAT]$_P$ | 0 | 10 | 20 |
| 0.0[a] | [b] | 305.3 | 317.5 |
| 0.1 | 316.8 ± 0.3 | 321.6 ± 0.4 | 320.8 ± 0.2 |
| 0.5 | 334.0 ± 0.2 | 331.3 ± 0.2 | 325.4 ± 0.4 |
| 1.0 | 335.9 ± 0.6 | 331.3 ± 0.2 | 327.5 ± 0.1 |

[a] From ref. 44. [b] Melted at room temperature.

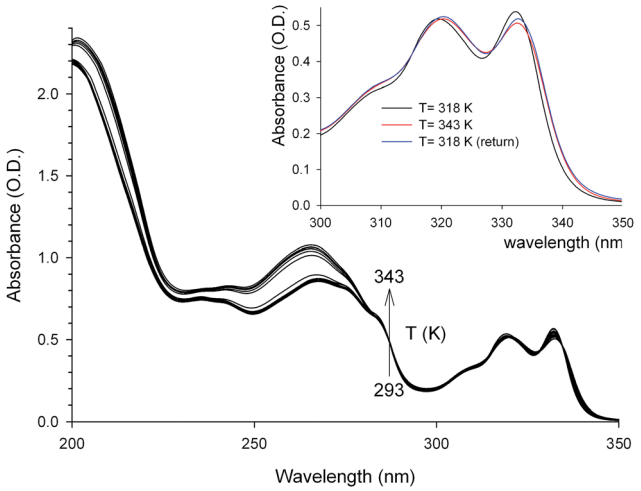


Fig. 10 UV spectra of the system **2**–polyAT ($R$ = 0.5) upon increasing the temperature. The inset shows the non reversibility of the melting process ([polyAT]$_P$ = 65.3 μM; $l$ = 1.0 cm).

on the series). The reversibility of the melting process was tested taking the samples back to a temperature well below $T_m$. At variance with the melting behaviour in the presence of complex **1**, while the CD spectra essentially recovered the initial pattern exhibited before heating, the UV-vis spectra in the region of $\lambda$ > 300 nm preserved the temperature-modified pattern (Fig. 10, inset) in the case of polyAT–complex **2** systems. No additional information could be obtained by fluorescence spectroscopy, since the nickel complex is non-fluorescent and the interaction with polyAT does not induce fluorescence.

The optimized geometry of the intercalation complex between [Ni(terpy)($H_2O$)$_2$Cl]$^+$ and the dodecanucleotide model of polyAT, obtained by QM/MM calculations, is shown in Fig. 11.

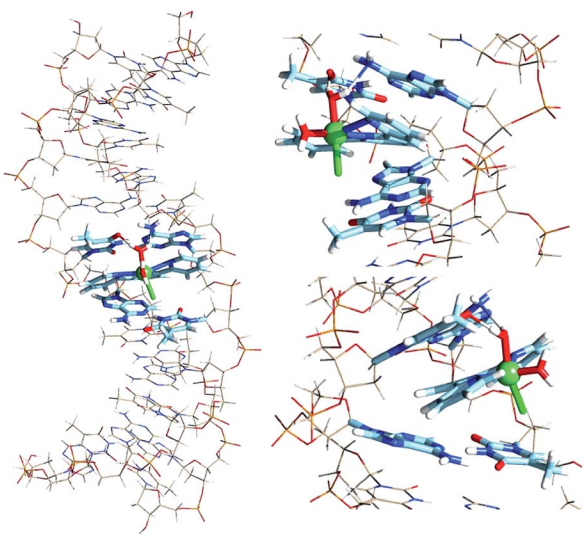

Fig. 11 Front and enlarged side views of the [Ni(terpy)($H_2O$)$_2$Cl]$^+$/d(ATATATATATAT)$_2$ intercalation complex, whose geometry was optimized by QM/MM calculations (2_dAT12.xyz; ESI†). High level and low level layers are shown as sticks and wires, respectively.

The presence of a chlorido ligand in apical position relative to the terpyridine plane, in the hexacoordinate geometry of the nickel ion in $[Ni(terpy)(H_2O)_2Cl]^+$, induces a remarkable increase of the size of the intercalation pocket, with consequent large axial elongation of the double helix. The hydrogen atoms of the apical water molecule of the nickel complex ion are hydrogen-bonded with the keto oxygen atom O4 of thymine and the amine nitrogen atom N6 of adenine.

## Discussion

The modifications caused by complex **1** on the CD spectra of polyAT, and to a lesser extent of polyGC, suggest a strong intercalative mechanism of interaction of the metal complex with the polynucleotide. The modifications of the UV-vis absorption spectra upon addition of the complex to polyAT (Fig. 1, inset) and to polyGC, even if less marked, are also normally observed only for intercalation, as noted in the Results section and in agreement with the literature.[32,36–38] Intercalative binding to polyAT is strongly supported also by the melting experiments results (Table 1). As expected, in the absence of complex **1**, $T_m$ increased with the salt concentration[32,44] while in the presence of $Cd(terpy)Cl_2$, $T_m$ was strongly dependent also on the value of $R$. It is well known[32,36,37,43,44] that intercalation induces a stabilization of the polynucleotide double helix, both by enhancement of the stacking interactions and by reduction of the charge density per unit length of the helix backbone due to the unwinding and stretching effects.[43] Indeed, $T_m$ increases regularly with $R$ for NaCl concentrations 0, 2 and 10 mM, supporting the importance of the proposed intercalative mechanism of interaction. The rise of $T_m$ with $R$ decreases with the increase of the salt concentration and $T_m$ appears to reach a limiting value of *ca.* 334–335 K. This limit is reached at $R$ values 0.7, 1.0, $\geq$1.5 for NaCl concentrations 0, 2 and 10 mM, respectively. This trend is in agreement with the increasing screening effect due to $Na^+$ cations, that stabilizes the double helix, hindering the access to the inner region and reducing the extent of intercalation or, more generally, of non-covalent interactions.[32,33] Such a screening effect is likely responsible of the weak increase of $T_m$ with $R$ found at the highest (20 mM) NaCl concentration. The attainment of a limiting $T_m$ value suggests saturation of all the sites of non-covalent stabilizing interactions. The seemingly irregular trend of $T_m$ with the salt concentration at constant $R$, would thus be the result of a complex balance of the two contrasting effects of the increasing ionic strength, *i.e.* the screening effect of the phosphate charge stabilizing the double helix, and the hindrance to the stabilizing intercalation process. Another puzzling feature is the abrupt decrease of $T_m$, recorded at the highest $R$ values for 0 and 2 mM NaCl concentrations (Table 1), suggesting that, under appropriate conditions, other types of interactions might occur, that destabilize the double helix, but the phenomenon was not further investigated.

QM/MM calculations indicate that intercalation of complex **1** in both the polyAT and the polyGC double helix is possible, though with structural differences that might be crucial (Fig. 4 and 5). Intercalation seems to be accompanied by additional stabilizing interactions, as hydrogen bonding between the chlorido ligands and the amine hydrogens of the nitrogen bases, as already mentioned. The short distances, found in the optimized geometry of the intercalation complexes, between the cadmium ion and the exocyclic carbonyl oxygens of either thymine or guanine (Cd–O distance 2.49 Å and 2.74 Å, respectively) would suggest the formation of an additional coordination bond of the cadmium ion. However this result, not supported by the experimental data, should be considered with caution, since the presence of solvent water was not explicitly taken into account in the calculations. The models indicate that the intercalation pocket in polyGC is smaller than in polyAT, implying a greater distortion of the polyAT double helix. The occurrence of an induced CD band, considerably larger for polyAT than for polyGC (Fig. 1 and 2), also indicates a tighter binding with the former polynucleotide, as suggested also by the fluorescence quenching experiments. Indeed, the Stern–Volmer constant in the case of polyAT ($k_{SV} = 1.5 \times 10^5\ M^{-1}$) is larger than in the case of polyGC ($k_{SV} = 6.3 \times 10^4\ M^{-1}$).

A special word of comment deserve the marked differences appearing between Fig. 2a and b, that were found to a lesser extent also for the polyAT–$Cd(terpy)Cl_2$ system. When $Cd(terpy)Cl_2$ was added to polyGC (Fig. 2a), the spectrum was progressively modified in the region at $\lambda$ < 300 nm when $R$ was increased and weak ICD signals developed at higher wavelengths ($\lambda$ in the range 300–350 nm). However, when polyGC was added to the complex (Fig. 2b) the growing CD spectrum increasingly resembled that of C- or unwound B-DNA and no sign of induced dichroism was observed. To try to rationalize a similar behaviour one should consider what happens in the course of the two experiments at a microscopic level. When polyGC (or polyAT) is titrated with $Cd(terpy)Cl_2$, the complex should statistically interact with the different double strands occupying first the higher affinity sites (intercalation) and only at higher $R$ values the other sites, if present. On the other hand, when $Cd(terpy)Cl_2$ is titrated with polyGC (or polyAT), the complex initially in large excess would occupy all the available sites on the duplex, causing possibly conspicuous conformational alterations. Further addition of polynucleotide should induce a redistribution of the complex among the newly available interaction sites. However, distribution among the different strands might not occur homogeneously and the already occurred modifications in the double helix might not be reversible. It is thus not unrealistic that samples of polynucleotide–$Cd(terpy)Cl_2$ at the same $R$ value, obtained with the two alternative procedures, are intrinsically different and the CD spectra would reflect real differences between samples only nominally identical.

It is, at this point, interesting to compare these results with those obtained with complex **2**. At variance with complex **1**, complex **2** bears a positive charge that favours its interaction with the negatively charged phosphate backbone of polyAT. Its octahedral geometry, while not inhibiting intercalation,[5,6,46] might favour partial intercalation or other types of non-covalent interaction. Indeed, also the calculated optimized geometry shows a large size of the intercalation pocket, with formation of hydrogen bonds and electrostatic interactions assisting the

 

intercalation process. It is, however reasonable the hypothesis of a bonding to polyAT weaker than that of complex **1**. The CD spectra exhibited conspicuous modifications on decreasing the value of $R$ (Fig. 8) suggesting strong interaction of the complex with the polynucleotide; however, at variance with complex **1**, only a very weak ICD signal at $\lambda > 300$ nm could be observed. A mechanism of partial intercalation stabilized by electrostatic interactions can be proposed to explain these features. The melting experiments (Table 2), on the other hand, confirmed the stabilization of the double helix induced by the complex **2**–polyAT interaction and the influence of the salt concentration on the interaction; comparison with the corresponding results obtained with complex **1** (Table 1) did not evidence substantial differences, thus supporting the intercalative nature of the binding. There are, however, some key differential features, the first of which is the lack of reversibility of the temperature-induced modifications for complex **2** already mentioned. Moreover, the progressive change exhibited by the UV-vis spectra in the case of complex **2**, suggests a gradual temperature-induced transformation of the bound complex to a somewhat different chemical species, unlike what was found with complex **1**. One of the major interaction mechanisms of metal complexes with polynucleotides involves formation of covalent bonds between the metal and the donor atoms of the nucleotides[8,46–49] following the hydrolysis of one or more labile ligands from the complex. Such mechanism is, for instance, basic for the antitumor activity of cis-platin.[50,51] In the present case of complex **2**, the increase of temperature would cause the substitution of one bound aqua ligand by one of the donor atoms of polyAT present in the minor groove and not involved in the W–C base pairing, *i.e.* C2 carbonyl of thymine and N3 of adenine. The presence of covalently bound nickel complex on the single strand polynucleotide after melting would not inhibit the transition, on cooling, to double helix, that would however present some distortions relative to the before-heating double helix, and thus exhibit modified CD and UV-vis spectra, as was indeed experimentally found.

# Experimental

### Chemicals

Terpyridine (Aldrich, >98%), ethanol (Baker, 95%), acetone (Carlo Erba *pro analysis*) were used as received. Tris-(2-amino-2(hydroxymethyl)-propan-1,3-diol) was a Sigma product. NaCl (Merck *suprapur*) was dried for 5 hours in the oven at 383 K and stored in a desiccator over silica gel. $NiCl_2 \cdot 6H_2O$ was a Carlo Erba *pro analysis* product (>98%) and $CdCl_2$ a Fluka reagent (>99%). PolyAT and polyGC (sodium salts) were Sigma products and ctDNA was from Fluka. PolyAT [MW = (0.9–1.9) $\times 10^6$ Da] was purchased in vials of 50 units and polyGC [MW = (4.9–5.2) $\times 10^5$ Da] in vials of 25 units. One unit is the amount of polynucleotide yielding an absorbance of 1.0 at 260 nm, when dissolved in 1.0 mL of water in a 1.0 cm optical pathlength cuvette. The lyophilized samples for the measurements were prepared in Eppendorf microvials from a stock solution of the two polymers according to a procedure previously described[44] and were stored over silica gel below 273 K.

### Instrumentation

CD spectra were recorded with a Jasco J715 spectropolarimeter under nitrogen flux; the temperature was controlled to $\pm 1$ K by means of a Julabo F10 thermostat.

UV-Vis spectra, at room temperature, were collected before each experiment with a double beam Varian Cary 100 spectrometer to obtain the actual concentration of polynucleotide in each sample. The concentration, expressed as molarity of phosphate groups, was calculated from the absorbance at 262 nm for polyAT and at 255 nm for polyGC (both corrected for the absorbance at 350 nm where no band is present), using $\varepsilon_{262} = 6650\ M^{-1}\ cm^{-1}$ for polyAT[52] and $\varepsilon_{255} = 8400\ M^{-1}\ cm^{-1}$ for polyGC.[53] The difference in polynucleotide content of nominally equal Eppendorf vials was never greater than 10%. Fluorescence spectra were recorded with a Fluoromax-2 Jobin Yvon-Spex spectrofluorimeter in the wavelength range 310–450 nm. Samples were excited at 280 nm with both excitation/emission slits set at 1.5 nm, with an integration time of 0.5 s. Stern–Volmer plots have been obtained by calculating the ratio $F_0/F$ from the fluorescence intensity at 350 nm for the complex **1** alone ($F_0$) and for the samples at increasing concentration of either polyAT and polyGC ($F$). Each emission intensity has been corrected for the absorbance of the samples at the excitation and the emission wavelengths.[45] For the fluorescence lifetime measurements, the experimental set-up is essentially the same already reported[31] except that a pulsed UV-LED emitting at 295 nm (PicoQuant, Germany) and a Hamamatsu R3809U-50 (Japan) detector have been used. In order to keep the S/N level constant among the different measurements, the same acquisition time has been used (typically, 600 s). For the IRF acquisition at 295 nm, 5 μL of a 30% Ludox (Sigma) solution were added directly in the cuvette at the end of each run of measurements. The fluorescence lifetime data were analysed by means of the FluoFit software (PicoQuant, Germany). Because of the acquisition strategy adopted, the total counts measured during any (fixed) acquisition time after each addition of polyAT and/or polyGC to solutions of the cadmium complex **1** (Scheme 1) have been used to draw a Stern–Volmer plot (insets of Fig. S8 and S9 – ESI†) to confirm the data coming from steady-state fluorescence measurements. In these cases, no correction for the solutions absorbance at the excitation and emission wavelengths was applied due both to their small values (well below 0.04 O.D. at 295 nm and close to zero at 350 nm) and to the lower sensitivity of the TCSPC technique to fluorophore concentration.[54]

Quartz Suprasil Hellma cuvettes (1.0 cm optical pathlength) were used for CD, UV-Vis and fluorescence spectra. Correction for dilution was always applied to the spectra, when pertinent.

IR spectra (KBr pellets) were collected with a Jasco FT/IR 420 instrument.

Elemental analyses for C, H and N were provided by the "Servizio di Microanalisi" of the Chemistry Department of the University of Roma "La Sapienza" (EA 1110 CHNS-O instrument).

A TGA Q5000 (TA Instruments) instrument was used for thermogravimetric analysis.

pH measurements were performed with a Crison GLP21 pH-meter using a combined type 52–51 electrode.

### Computational details

The coordinates of two alternating deoxydodecanucleotide duplexes, $d(ATATATATATAT)_2$ and $d(GCGCGCGCGCGC)_2$, in the B-DNA conformation and presenting an intercalation pocket between the sixth and seventh base pairs, have been taken from our previous studies.[55,56] For the nickel complex **2** (Fig. 1), the X-ray determined structure,[24] with two *cis* water molecules in the coordination sphere of the nickel cation, $[Ni(terpy)(H_2O)_2Cl]^+$, was used in the calculations. The geometry of the intercalation complexes was optimized by two-layer QM/MM calculations, as implemented in the ONIOM method,[57,58] with the aim to perform a high-level calculation on the intercalation pocket and to take account of the constraining effects of the double-helical structure at lower levels of theory. The energy values of the optimized geometries are reported in Table S4 of ESI.† The M06-2X[59] DFT functional and the Lanl2dz pseudopotential basis set[60] were used in the higher QM layer, to suitably model the hydrogen bonding and π–π stacking interactions between the sixth and seventh Watson–Crick base pairs. The Amber99 force field was used in the lower MM layer of the DFT/MM calculations, as recently described.[55,56] The highest layer of the model includes the sixth and seventh base pairs and the two metal complexes. Default atomic partial charges were used for the dodecanucleotide atoms, implicitly included in the force field parameters. Vibration frequency calculations, within the harmonic approximation, where performed to confirm that the two optimized geometries represented a minimum in the potential energy surface.

## Conclusions

The "computational microscope"[61] represented by quantum chemical modelling and experimental techniques are highly complementary in the study of DNA–drug interactions.[62] Indeed, we may conclude that in our study the joint use of experimental and computational techniques has been the decisive approach to unravel the details of the interactions between polynucleotides and both terpyridine complexes at molecular level, even though some details remain to be clarified. All the experimental data indicate a binding of Cd(terpy)$Cl_2$ to polyAT tighter than to polyGC, even though not selective as indicated by the binding also to ctDNA. In both cases, the interaction is strong and intercalative. Even in the case of the $[Ni(terpy)(H_2O)_2Cl]^+$ complex cation, the experimental results point to an intercalative mode of binding. Recently, a fascinating and new way of interaction of metal complexes with DNA has been proposed in the literature, based on theoretical[62] and experimental evidences.[63] This mode of binding is indicated as eversion or insertion, and implies the ejection from the B-DNA double helix of one base pair substituted by the metal–complex species. Even though in our case the experimental data do not allow to rule out such hypothesis, it seems very unlikely. In fact, in all the documented cases, the insertion point is represented by a thermodynamically destabilized mismatched site,[64] that in the synthetic copolymers used in our work is absent or present in an extremely small mole fraction, that cannot alter the spectroscopic evidences here reported.

In the case of the complex **1**–polyAT system, the lack of experimental evidences of a sixth coordination bond of the metal, suggested by the short distances obtained by QM/MM calculations, can be ascribed either to an extremely labile bond not leading to the formation of a stable chemical species, or to the need of slightly improved computational models taking into consideration, for example, explicit solvent water molecules that could modulate the complex **1**–polyAT interaction. In any case, even the QM/MM calculation results support the stronger interaction of **1** with polyAT.

## Acknowledgements

A special thank is deserved to Profs. G. Palazzo (University of Bari – Italy) and K. Shillen (University of Lund – Sweden) for critical reading of the manuscript in its final form. Financial support of Palermo and Rome "La Sapienza" Universities is gratefully acknowledged. M. G. thanks C.S.G.I. (O.U. of Bari, Italy) for partial financial support.

## Notes and references

1 C. Metcalfe and J. A. Thomas, *Chem. Soc. Rev.*, 2003, **32**, 215.
2 R. Blasius, C. Moucheron and A. Kirsch-de Maesmaker, *Eur. J. Inorg. Chem.*, 2004, **2004**, 3971.
3 L. J. K. Boerner and J. M. Zaleski, *Curr. Opin. Chem. Biol.*, 2005, **9**, 135.
4 M. T. Carter, M. Rodriguez and A. J. Bard, *J. Am. Chem. Soc.*, 1989, **111**, 8901.
5 *Metal complex-DNA interactions*, ed. N. Hadjiliadis and E. Sletten, Wiley-Blackwell, Chichester, 2009.
6 H.-K. Liu and P. J. Sadler, *Acc. Chem. Res.*, 2011, **44**, 349.
7 G. T. Morgan and F. H. Burstall, *J. Chem. Soc.*, 1932, 20.
8 S. D. Cummings, *Coord. Chem. Rev.*, 2009, **253**, 1495.
9 C.-W. Jiang, H. Chao, H. Li and L.-N. Ji, *J. Inorg. Biochem.*, 2003, **93**, 247.
10 V. Uma, M. Elango and B. U. Nair, *Eur. J. Inorg. Chem.*, 2007, **2007**, 3484.
11 U. S. Schubert, H. Hofmeier and G. R. Newkome, *Modern terpyridine chemistry*, Wiley-VCH, Weinheim, 2006.
12 S. Rajalakshmi, T. Weyhermüller, M. Dinesh and B. U. Nair, *J. Inorg. Biochem.*, 2012, **117**, 48.
13 M. Airoldi, G. Gennaro, M. Giomini, A. M. Giuliani and M. Giustini, *J. Biomol. Struct. Dyn.*, 2007, **25**, 77.
14 M. Airoldi, G. Gennaro, M. Giomini, A. M. Giuliani and M. Giustini, *Chirality*, 2008, **20**, 951.
15 M. Airoldi, G. Gennaro, M. Giomini, A. M. Giuliani, M. Giustini and G. Palazzo, *Phys. Chem. Chem. Phys.*, 2011, **13**, 12293.
16 G. Morgan and F. H. Burstall, *J. Chem. Soc.*, 1937, 1649.
17 D. E. C. Corbridge and E. G. Cox, *J. Chem. Soc.*, 1956, 594.
18 C. M. Harris, T. N. Lockyer and N. C. Stephenson, *Aust. J. Chem.*, 1966, **19**, 1741.

 

19 J. Pickardt, B. Staub and K. O. Schäfer, *Z. Anorg. Allg. Chem.*, 1999, **625**, 1217.
20 N. W. Alcock, P. R. Barker, J. M. Haider, M. J. Hannon, C. L. Painting, Z. Pikramenou, E. A. Plummer, K. Rissanen and P. Saarenketo, *J. Chem. Soc., Dalton Trans.*, 2000, 1447.
21 M. A. R. Meier, B. G. G. Lohmeijer and U. S. Schubert, *J. Mass Spectrom.*, 2003, **38**, 510.
22 S. Bode, R. K. Bose, S. Matthes, *et al.*, *Polym. Chem.*, 2013, **4**, 4966.
23 R. Hogg and R. J. Wilkins, *J. Chem. Soc.*, 1962, 341.
24 R. Cortés, M. I. Arriortua, T. Rojo, X. Solans, C. Miravitlles and D. Beltran, *Acta Crystallogr., Sect. C: Struct. Chem.*, 1985, **41**, 1733.
25 J. S. Judge and W. A. Baker Jr, *Inorg. Chim. Acta*, 1967, **1**, 239.
26 C. M. Harris and T. N. Lockyer, *Aust. J. Chem.*, 1970, **23**, 1703.
27 F. Lions, I. G. Dance and J. Lewis, *J. Chem. Soc. A*, 1967, 565.
28 J. S. Judge, W. M. Reiff, G. M. Intille, P. Ballway and W. A. Baker Jr, *J. Inorg. Nucl. Chem.*, 1967, **29**, 1711.
29 M. Chiper, S. Hoeppener, U. S. Schubert, C.-A. Fustin and J.-F. Gohy, *Macromol. Chem. Phys.*, 2010, **211**, 2323 and refs therein.
30 M. Chiper, M. A. R. Meier, D. Wouters, S. Hoeppener, C.-A. Fustin, J.-F. Gohy and U. S. Schubert, *Macromolecules*, 2008, **41**, 2771.
31 M. Airoldi, G. Barone, G. Gennaro, A. M. Giuliani and M. Giustini, *Biochemistry*, 2014, **53**, 2197.
32 M. Cusumano, M. L. Di Pietro, A. Giannetto and P. A. Vainiglia, *J. Inorg. Biochem.*, 2005, **99**, 560.
33 M. Cusumano, M. L. Di Pietro, A. Giannetto and P. A. Vainiglia, *Inorg. Chem.*, 2007, **46**, 7148.
34 S. Allenmark, *Chirality*, 2003, **15**, 409.
35 M. Ardhammar, B. Norden and T. Kurucsev, in *Circular dichroism – principles and applications*, ed. N. Berova, K. Nakanishi and R. W. Woody, Wiley-VCH, New York, 2nd edn, 2000, pp. 741–768.
36 C. V. Kumar and E. H. Asuncion, *J. Am. Chem. Soc.*, 1993, **115**, 8547.
37 R. B. Nair, E. S. Teng, S. L. Kirkland and C. J. Murphy, *Inorg. Chem.*, 1998, **37**, 139.
38 C. V. Kumar, E. H. A. Punzalan and W. B. Tan, *Tetrahedron*, 2000, **56**, 7027.
39 S. Hanlon, S. Brudno, T. T. Wu and B. Wolf, *Biochemistry*, 1975, **14**, 1648.
40 W. A. Baase and W. C. Johnson Jr, *Nucleic Acids Res.*, 1979, **6**, 797.
41 C. A. Sprecher, W. A. Baase and W. C. Johnson, *Biopolymers*, 1979, **18**, 1009.
42 F. Cui, R. Huo, G. Hui, X. Lv, J. Jin, G. Zhang and W. Xing, *J. Mol. Struct.*, 2011, **1001**, 104.
43 M. T. Bjorndal and D. K. Fygenson, *Biopolymers*, 2002, **65**, 40.
44 M. Airoldi, C. A. Boicelli, G. Gennaro, M. Giomini, A. M. Giuliani and M. Giustini, *Phys. Chem. Chem. Phys.*, 2000, **2**, 4636.
45 T. D. Gauthier, E. C. Shane, W. F. Guerin, W. R. Seitz and C. L. Grant, *Environ. Sci. Technol.*, 1986, **20**, 1162.
46 R. Žaludová, V. Kleinwächter and V. Brabec, *Biophys. Chem.*, 1996, **60**, 135.
47 C. S. Peyratout, T. K. Aldridge, D. K. Crites and D. R. McMillin, *Inorg. Chem.*, 1995, **34**, 4484.
48 P. M. van Vliet, S. M. S. Toekimin, J. G. Haasnoot, J. Reedijk, O. Nováková, O. Vrána and V. Brabec, *Inorg. Chim. Acta*, 1995, **231**, 57.
49 O. Nováková, J. Kašpárková, O. Vrána, P. M. van Vliet, J. Reedijk and V. Brabec, *Biochemistry*, 1995, **34**, 12369.
50 *Metallopharmaceuticals-I-DNA interactions*, ed. M. J. Clarke and P. J. Sadler, Springer, Berlin, 1999.
51 J. K.-C. Lau and B. Ensing, *Phys. Chem. Chem. Phys.*, 2010, **12**, 10348.
52 R. B. Gennis and C. R. Cantor, *J. Mol. Biol.*, 1972, **65**, 381.
53 F. E. Rossetto and E. Nieboer, *J. Inorg. Biochem.*, 1994, **54**, 167.
54 Y. Chen and A. Periasamy, *Microsc. Res. Tech.*, 2004, **63**, 72.
55 A. Lauria, R. Bonsignore, A. Terenzi, A. Spinello, F. Giannici, A. Longo, A. M. Almerico and G. Barone, *Dalton Trans.*, 2014, **43**, 6108.
56 A. Spinello, A. Terenzi and G. Barone, *J. Inorg. Biochem.*, 2013, **124**, 63.
57 M. Svensson, S. Humbel, R. D. J. Froese, T. Matsubara, S. Sieber and K. Morokuma, *J. Phys. Chem.*, 1996, **100**, 19357.
58 T. Vreven and K. Morokuma, *J. Comput. Chem.*, 2000, **21**, 1419.
59 Y. Zhao and D. G. Truhlar, *Theor. Chem. Acc.*, 2008, **120**, 215.
60 P. J. Hay and W. R. Wadt, *J. Chem. Phys.*, 1985, **82**, 270.
61 E. H. Lee, J. Hsin, M. Sotomayor, G. Comellas and K. Schulten, *Structure*, 2009, **17**, 1295.
62 E. Dumont and A. Monari, *J. Phys. Chem. Lett.*, 2013, **4**, 4119.
63 C. Cordier, V. C. Pierre and J. K. Burton, *J. Am. Chem. Soc.*, 2007, **129**, 12287.
64 B. M. Zeglis, V. C. Pierre and J. K. Barton, *Chem. Commun.*, 2007, 4565.